

Realistic Simulation of Breast Tissue Microstructure in Software Anthropomorphic Phantoms

Predrag R. Bakic,¹ David D. Pokrajac,²
Raffaele De Caro,³ and Andrew D.A. Maidment¹

¹ Dept. of Radiology, University of Pennsylvania, Philadelphia, PA, USA

² Computer and Information Sciences Dept., Delaware State University, Dover, DE, USA

³ Dept. of Human Anatomy and Physiology, University of Padova, Italy

Predrag.Bakic@uphs.upenn.edu

Abstract. Software anthropomorphic breast phantoms have been used in virtual clinical trials for preclinical validation of breast imaging systems. Virtual trial quality depends largely on the realism of the simulated breast anatomy. Our phantom design has been focused on the simulation of large-scale and meso-scale anatomical structures, including the breast outline, skin, and matrix of Cooper's ligaments and tissue compartments. Realism of such a design has been confirmed in comparative studies of phantom and clinical power spectra and parenchymal texture. We present a novel method for simulating the hierarchical organization of breast tissue subcompartments, seen in detailed histological images. The subcompartmentalization introduces microstructure in breast phantoms, resulting in improved realism of phantom images. The qualitative validation of phantoms with simulated microstructure is discussed in this paper; the quantitative validation is ongoing.

Keywords: Software breast phantoms, virtual clinical trials, small-scale tissue simulation, stereology, testing realism.

1 Introduction

Virtual clinical trials (VCTs) have received considerable attention recently; a VCT is an efficient way to perform optimization and preclinical validation of novel breast imaging systems (1, 2). VCTs are based upon sophisticated computer simulations of breast anatomy, image acquisition, image processing and display. The synthetic images generated by VCT can be assessed by model or human observers.

The quality of a VCT depends upon a number of factors including phantom realism; the phantom realism needs to be commensurate with the diagnostic task in question. The University of Pennsylvania (UPenn) breast anatomy model is based upon the simulation of large-scale and meso-scale anatomical structures; a variety of features are modelled, including the overall breast outline, the skin, the matrix of Cooper's ligaments and tissue compartments, and the assignment of adipose and fibroglandular tissue to these compartments.(3) The validity of this design has been confirmed for a number of tasks, and the visual realism of the anatomy model is

supported by a number of comparative studies of phantom and clinical power spectra (4, 5) and parenchymal texture (6-8).

That said, we are constantly striving to improve the breast anatomy model further. In this paper, we present a novel method for simulating the hierarchical organization of breast tissue subcompartments, seen in detailed histological images. The introduction of a hierarchy of subcompartments into our breast anatomy model results in more realistic phantom images.

2 Methods

2.1 Histological Analysis

Our existing method for simulating breast tissue structures was motivated by the observed appearance of tissue compartments in existing histology and computed tomography breast images. In this paper we present a new analysis of histology slices from two breasts specimens; one obtained after breast reduction and another after mastopexy. The patients were aged 33 and 50, respectively. No abnormalities were detected in the two analysed breast specimens. The histologic analysis was performed at the University of Padova, Italy. Ten histology slices were analysed, at least one slice from each breast quadrant.

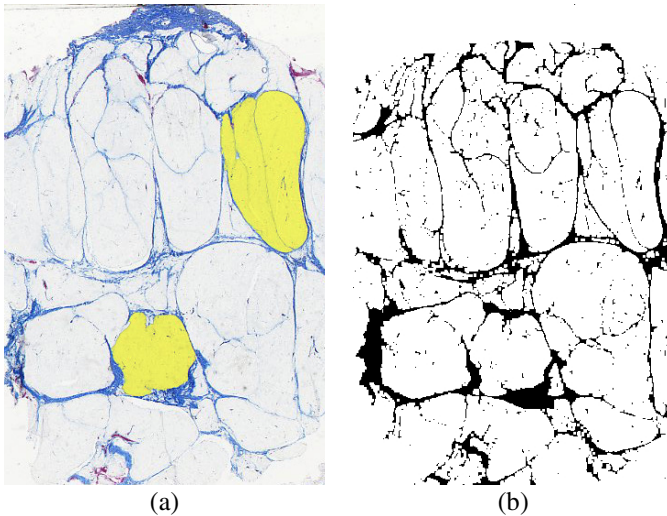


Fig. 1. An example of a breast histology image used in the size and shape analysis of adipose tissue compartments: (a) histology section with the Azan-Mallory staining; two analysed compartments are highlighted; (b) a binarized version of the same histology section

Fig. 1(a) shows a detailed microscopic image of the breast obtained using Azan-Mallory staining. The Azan-Mallory staining technique combines the original Mallory

connective tissue stain with azocarmine (9); as a result, collagen is stained blue, nuclei and cytoplasm are red, and elastic fibres are pink or unstained. The section in Fig. 1(a) is oriented so that the areolar region is superior. In this example, the adipose tissue compartments are clearly encapsulated by the blue stained Cooper's ligaments. Two individual compartments have been highlighted to illustrate this observation.

Digital images of the stained histologic slices were binarized by thresholding. A binarized image of the matching tissue section is shown in Fig. 1(b). The binarized sections were used to estimate the size and shape of the tissue compartments. Two parameters, mean volume and axial ratio, were calculated using the stereological unfolding method by Saltykov, which assumes an ellipsoidal compartment shape (10). From this, compartment size and shape distributions were calculated.

Examination of Fig. 1 suggests that the thickness of the Cooper's ligaments depends upon the volume of the associated compartments. Thus, we have also estimated the volumetric fraction of the connective tissue and the average thickness of the Cooper's ligaments.

Finally, as seen in Fig. 1(a), the individual adipose compartments appear to be divided into smaller compartments by interlobular fibrous septa. Due to their small thickness, these interlobular fibrous septa may not be clearly visible in clinical breast images; however, they certainly contribute to the small-scale tissue variations seen in clinical images. The combination of the thicker Cooper's ligaments and the thinner interlobular fibrous septa indicate a hierarchical organization of tissue compartments. This observation has motivated the modification of our breast anatomy model.

2.2 Computer Simulation

In order to increase the realism of our breast anatomy model, we have included a simulation of subcompartments with septa of reduced thickness. We begin by simulating a baseline phantom, P , containing large compartments and correspondingly thick ligaments. We then simulate a second subcompartment phantom, S , having the same size and outline as the baseline phantom, containing smaller compartments and thinner ligaments; the internal structure of the second phantom will form the structure of the subcompartments. The final phantom is obtained by superimposing the subcompartment phantom on the baseline phantom. Algorithmically, a voxel $v_p(x,y,z)$ of P at spatial coordinate x,y,z is replaced by the corresponding voxel $v_s(x,y,z)$ of S if and only if $v_s(x,y,z)$ is part of a ligament in S , and $v_p(x,y,z)$ belongs to a compartment in P .

We tested this method with a set of preliminary models in which each compartment in P was divided on average into thirty subcompartments. In this test, we simulated baseline phantoms with 333 compartments and subcompartment phantoms with 10,000 compartments. The simulated thickness of the interlobular fibrous septa was selected to be $200\mu\text{m}$ in the subcompartment phantoms, 3 times smaller than the $600\mu\text{m}$ thickness of the primary Cooper's ligaments in the baseline phantoms.

The simulated microstructure was assessed subjectively based upon synthetic mammographic projections of phantoms with or without subcompartments. The synthetic images were generated using the breast anatomy and imaging simulation

pipeline, developed at the University of Pennsylvania for the purpose of conducting VCTs of breast imaging systems (1). The pipeline includes modules for the simulation of normal breast anatomy, insertion of lesions, breast positioning and deformation, clinical image acquisition, image reconstruction and post-processing, image display, and image interpretation by model observers. External modules may be included in the pipeline as plugins.

The software breast phantoms with and without subcompartments were subject to simulated mammographic compression using a finite element deformation method (11). Mammographic imaging was then simulated using a ray tracing projection method, assuming a poly-energetic x-ray beam without scatter, and an ideal detector model. The quantum noise was simulated by adding a random Poisson process. The simulated image acquisition geometry corresponds to the Hologic Selenia Dimensions full-field digital mammography system (Hologic Inc., Bedford, MA). The resulting synthetic raw projections are post-processed using a commercial software package (Adara, Real Time Tomography, Villanova, PA).

3 Results and Discussion

3.1 Histological Analysis

Table 1 gives the values of average compartment volume, axial ratios and ligament thickness, as estimated from histology slides, in three different regions of the breast: subcutaneous (“Sub-Q”), posterior, and periglandular. These values have been averaged over 30 analysed adipose compartments. Adipose tissue compartments have a larger volume in the subcutaneous (0.84 ml) and posterior (0.94 ml) regions, as compared to the periglandular region (0.26 ml). Visually, these estimates of compartment volume agree with the observed appearance of breast tissue structures in these regions of clinical images.

The orientation of the breast tissue compartments had relatively little dependence upon region; the axial ratio varied from 2.02 in the subcutaneous region to 2.91 in the posterior region. This range of axial ratios corresponds to an angular difference of just 7 degrees. The variation in angular ratios is considerably larger in the posterior region (0.30; i.e., 10% of the average angular ratio), as compared to the subcutaneous region (0.14; 6%) and periglandular region (0.12; 6%). This suggests that some underlying structure may exist in these areas, which constrains the shape and orientation of the compartments.

Table 2 shows the volume fraction and thickness of the connective tissue, estimated from the binarized images of the stained Cooper’s ligaments. The tabulated values have been averaged over 10 analysed tissue slices. The estimated average volume fraction was 12.3%, while the average thickness of Cooper’s ligaments was 289 μm . The estimated ligament thickness fits well within the range of thicknesses used in our previous computer simulation of Cooper’s ligaments: 200-600 μm . The volume fraction showed 11% variation relative to the mean value, while the ligament thickness showed 5% variation relative to the mean value.

Table 1. Average values of compartment volumes and axial ratios in various breast regions, estimated from breast histological sections

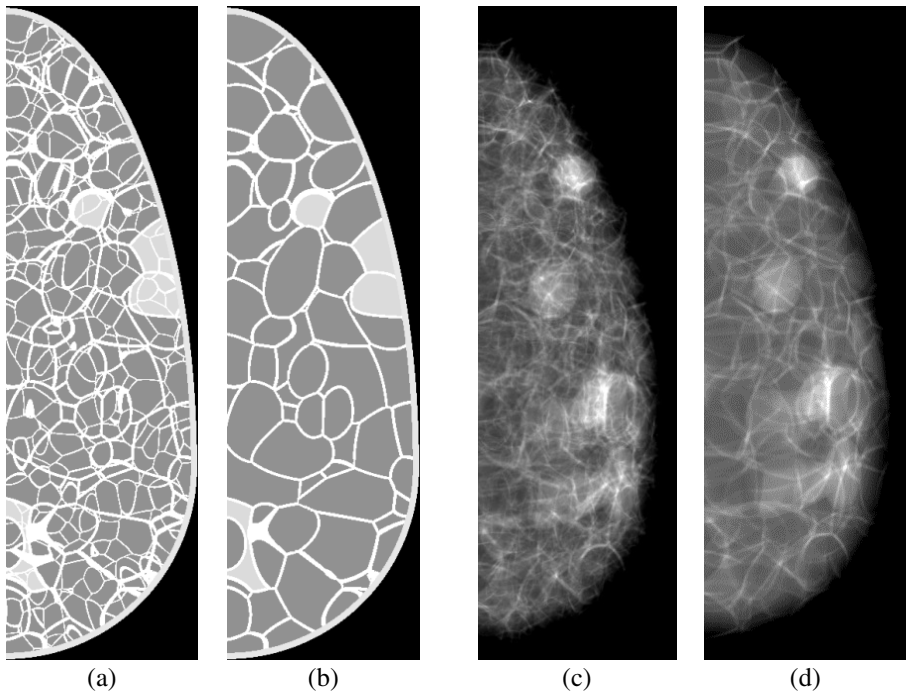
Region	Volume (cm ³)	Axial ratio
Sub-Q	0.84 ± 0.04	2.02 ± 0.14
Posterior	0.94 ± 0.07	2.91 ± 0.30
Periglandular	0.26 ± 0.01	2.04 ± 0.12

Table 2. Average values of the connective tissue volume fraction and thickness, estimated from Cooper's ligaments in breast histological sections

	Volume fraction (%)	Thickness (μm)
Cooper's ligaments	12.3 ± 1.4	289.2 ± 13.0

3.2 Computer Simulation

Fig. 2 shows preliminary results of the simulation of subcompartments in a breast phantom. Fig. 2(a) show a cross-section of a baseline phantom simulated with

**Fig. 2.** Simulation of breast tissue microstructure by subcompartmentalization. Shown are sections of a software phantom (a) with and (b) without subcompartments, with corresponding synthetic mammographic projections (c) with and (d) without subcompartments.

subcompartments, while Fig. 2(b) shows the same phantom without subcompartments. Figs. 2(c-d) show the corresponding synthetic mammographic projections of these phantoms. In both cases, the phantoms have a total volume of 450 cm^3 , with $100 \mu\text{m}$ voxels. Subjectively, the projection image of the subcompartmentalized phantom shows a higher level of realism. The simulated parenchymal pattern is enriched by the addition of small-scale structures. In addition, the simulated Cooper's ligaments appear less prominent and less geometric, as compared to the projection of the phantom without subcompartments.

A quantitative analysis was performed by comparison of the Laplacian Fractional Entropy (LFE) in clinical and synthetic images. The LFE measure describes the relative content of non-Gaussian statistics in breast images (12). The LFE analysis of the phantoms confirmed that the addition of subcompartments yields a considerable improvement in the LFE measure; the phantom with subcompartments is much closer to clinical images (8). The results of the LFE analysis are shown in Fig. 3. At low spatial frequencies, the phantom without subcompartments exceeds the LFE estimated in clinical mammograms. The peak LFE value of 92% occurs at 0.35 cyc/mm . At spatial frequencies above this peak, the LFE drops to zero at 1.0 cyc/mm . Subcompartmentalization reduces the LFE values, thus matching closely those estimated in mammograms. Based upon our current simulation method, subcompartmentalization increases the simulation time proportional to the square root of the number of compartments. This may be potentially prohibitive for real-time VCT simulations. As a viable alternative, we could pre-compute a number of subcompartment phantoms to be combined randomly with baseline phantoms created in real time.

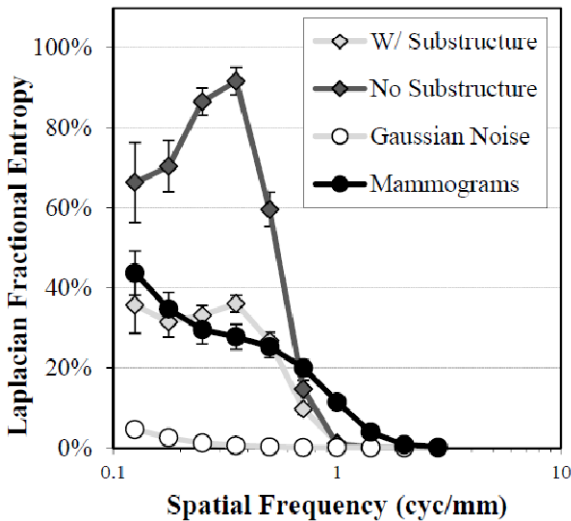


Fig. 3. Laplacian Fractional Entropy (LFE) as a function of spatial frequency, estimated from phantoms generated with and without subcompartments. The phantom LFE values are shown in comparison with those estimated from clinical mammograms and simulated Gaussian noise. Error bars show ± 1 standard deviation. (Reproduced with permission from Ref. #8.)

Our future work will include a more detailed analysis of phantoms containing sub-compartments, and a more complete exploration of the various simulation parameters for each of the tissue regions analysed in this work (subcutaneous, deep, and periglandular). In this way, we hope to add spatial dependence to our anatomy simulation method, further improving realism.

4 Conclusions

We have simulated the microstructure of breast tissue by adding subcompartments to our current design of anthropomorphic breast phantoms. This modification was motivated by the hierarchical organization of Cooper's ligaments and interlobular fibrous septa, as shown by Azan-Mallory stained breast histologic slices.

Subjectively, synthetic images of phantoms with subcompartmentalization show an improved level of realism; the simulated parenchymal pattern has been enriched, while the simulated Cooper's ligaments appear less geometric. The observed improvement in the appearance of phantom images is in agreement with a preliminary quantitative validation based upon Laplacian Fractional Entropy analysis.

Acknowledgements. This work was supported in part by the US National Institutes of Health (R01 grant #CA154444), the US Department of Defense Breast Cancer Research Program (HBCU Partnership Training Award #BC083639), the US National Science Foundation (CREST grant #HRD-0630388 and III grant # 0916690), and the US Department of Defense/Department of Army (45395-MA-ISP, #54412-CI-ISP, W911NF-11-2-0046), and the Delaware IDeA Network of Biomedical Research Excellence award. The content is solely the responsibility of the authors and does not necessarily represent the official views of the NIH, NSF and DoD. The authors are thankful to Drs. Veronica Macchi, Andrea Porzionato, and Cesare Tiengo from the University of Padova for preparing histological breast slides and performing the stereological analysis, and to Ms. Susan Ng from Real-Time Tomography (Villanova, PA) for processing simulated projection images. ADAM is a scientific advisor to Real-Time Tomography.

References

1. Maidment, A.D.A., Bakic, P.R., Chui, J.H., Avanaki, A.N., Marchessoux, C., Pokrajac, D.D., et al.: The Role of Virtual Clinical Trials in Preclinical Testing of Breast Imaging Systems. In: 99th RSNA Scientific Assembly and Annual Meeting. RSNA, Chicago (2013)
2. Bakic, P.R., Myers, K.J., Reiser, I., Kiarashi, N., Zeng, R.: Virtual Tools for Validation of X-Ray Breast Imaging Systems. *Medical Physics* 40(6), 390 (2013)
3. Pokrajac, D.D., Maidment, A.D.A., Bakic, P.R.: Optimized generation of high resolution breast anthropomorphic software phantoms. *Medical Physics* 39(4), 2290–2302 (2012)
4. Bakic, P.R., Lau, B., Carton, A.-K., Reiser, I., Maidment, A.D.A., Nishikawa, R.M.: An Anthropomorphic Software Breast Phantom for Tomosynthesis Simulation: Power Spectrum Analysis of Phantom Projections. In: Martí, J., Oliver, A., Freixenet, J., Martí, R. (eds.) *IWDM 2010*. LNCS, vol. 6136, pp. 452–458. Springer, Heidelberg (2010)

5. Lau, A.B., Bakic, P.R., Reiser, I., Carton, A.-K., Maidment, A.D.A., Nishikawa, R.M.: An Anthro-pomorphic Software Breast Phantom for Tomosynthesis Simulation: Power Spectrum Analysis of Phantom Reconstructions. *Medical Physics* 37, 3473 (2010)
6. Kontos, D., Bakic, P.R., Carton, A.-K., Troxel, A.B., Conant, E.F., Maidment, A.D.A.: Parenchymal Pattern Analysis in Digital Breast Tomosynthesis: Towards Developing Imaging Biomarkers of Breast Cancer Risk. *Academic Radiology* 16(3), 283–298 (2008)
7. Bakic, P.R., Keller, B., Zheng, Y., Wang, Y., Gee, J.C., Kontos, D., et al.: Testing Realism of Software Breast Phantoms: Texture Analysis of Synthetic Mammograms. In: Nishikawa, R.M., Whiting, B.R., Hoeschen, C. (eds.) *SPIE Physics of Medical Imaging*, vol. 8668. SPIE, Lake Buena Vista (2013)
8. Abbey, C.K., Bakic, P.R., Pokrajac, D.D., Maidment, A.D.A., Eckstein, M.P., Boone, J.M.: Non-Gaussian Statistical Properties of Virtual Breast Phantoms. In: Mello-Thoms, C.R., Kupinski, M.A. (eds.) *SPIE Image Processing, Observer Performance, and Technology Assessment*. SPIE, San Diego (2014)
9. Bergman, R.A.: *Anatomy Atlases; A digital library of anatomy information*, <http://www.anatomyatlases.org/> (cited March 8, 2014)
10. Weibel, E.R.: *Stereological Methods*. Academic Press, London (1979)
11. Lago, M.A., Maidment, A.D.A., Bakic, P.R.: Modelling of mammographic compression of anthropomorphic software breast phantom using FEBio. In: *Int'l Symposium on Computer Methods in Biomechanics and Biomedical Engineering*. UT 2013, Salt Lake City (2013)
12. Abbey, C.K., Nosrateih, A., Sohl-Dickstein, J., Yang, K., Boone, J.M.: Non-Gaussian statistical properties of breast images. *Medical Physics* 39, 7121–7130 (2012)